An evaluation of different forest cover geospatial data for riparian shading and river temperature modelling

Dugdale, Stephen J.; Hannah, David M.; Malcolm, Iain A.

DOI:
10.1002/rra.3598

Citation for published version (Harvard):
Dugdale, SJ, Hannah, DM & Malcolm, IA 2020, 'An evaluation of different forest cover geospatial data for riparian shading and river temperature modelling', *River Research and Applications*, vol. 36, no. 5, pp. 709-723. https://doi.org/10.1002/rra.3598

Received: 13 July 2019 | Revised: 25 November 2019 | Accepted: 2 January 2020
DOI: 10.1002/rra.3598

RESEARCH ARTICLE

WILEY

An evaluation of different forest cover geospatial data for riparian shading and river temperature modelling

Stephen J. Dugdale[1,2] | David M. Hannah[2] | Iain A. Malcolm[3]

[1]School of Geography, University of Nottingham, University Park, Nottingham, UK
[2]School of Geography, Earth and Environmental Sciences, University of Birmingham, Birmingham, UK
[3]Marine Scotland Science, Freshwater Fisheries Laboratory, Pitlochry, UK

Correspondence
Stephen J Dugdale, School of Geography, University of Nottingham, University Park, Nottingham NG7 2RD, UK.
Email: stephen.dugdale@nottingham.ac.uk

Funding information
H2020 Marie Skłodowska-Curie Actions, Grant/Award Number: 702468

Abstract

Riparian tree planting is increasingly being used as a strategy to shade river corridors and offset the impact of climate change on river temperature. Because the circumstances under which tree planting generates the greatest impact are still largely unknown, researchers are increasingly using process-based models to simulate the impacts of tree planting (or felling) on river temperature. However, the high-resolution data on existing riparian tree cover needed to parameterise these models can be difficult to obtain, especially in data-sparse areas. In this paper, we compare the performance of a river temperature model parameterised with a range of different tree cover datasets, to assess whether tree cover data extracted from readily available GIS databases or coarser (i.e., 2–5 m) digital elevation products are able to generate river temperature simulations approaching the accuracy of higher resolution structure from motion (SfM) or LiDAR. Our results show that model performance for simulations incorporating these data is generally degraded in relation to LiDAR/SfM inputs and that tree cover data from "alternative" sources can lead to unexpected temperature model outcomes. We subsequently use our model to simulate the addition/removal of riparian tree cover from alongside the river channel. Simulations indicate that the vast majority of the "shading effect" is generated by tree cover within the 5-m zone immediately adjacent to the river channel, a key finding with regards to developing efficient riparian tree planting strategies. These results further emphasise the importance of incorporating the highest possible resolution tree cover data when running tree planting/clearcutting scenario simulations.

KEYWORDS
climate change, forest cover, geospatial data, process-based model, riparian shade, river temperature

1 | INTRODUCTION

There is increasing concern that climate change could alter the suitability of rivers for socio-economically important fish species, in particular salmonids which are adapted to cold water environments (Ficke, Myrick, & Hansen, 2007; Isaak, Wollrab, Horan, & Chandler, 2012; Jonsson & Jonsson, 2009). It is increasingly accepted that riparian woodland reduces the sensitivity of rivers to climate forcing and is a potentially valuable climate mitigation measure (Battin et al., 2007; Bowler, Mant, Orr, Hannah, & Pullin, 2012; Hannah, Malcolm, Soulsby, & Youngson, 2008; Seixas, Beechie, Fogel, & Kiffney, 2018). However, the circumstances and geographical context under which riparian woodland has the greatest impact on stream temperature are less well understood. One of the ways in which researchers are currently addressing this lack of knowledge is through the use of process-based models that simulate river temperature as a function of input meteorological

This article is published with the permission of the Controller of HMSO and the Queen's Printer for Scotland.

(e.g., air temperature, humidity, and solar radiation) and hydromorphic (e.g., discharge, basin topography, and channel morphology) data. Although the majority of these input variables are relatively straightforward to measure in the field or can be derived from meteorological databases or GIS repositories, some of the information required to run river temperature models can be more difficult to obtain. This is particularly the case for data characterising riparian tree cover. To provide accurate stream temperature predictions in tree-covered reaches, many stream temperature models contain routines capable of simulating this effect, given appropriate data on riparian tree cover and height (see Dugdale, Hannah, & Malcolm, 2017). However, the availability, quality and source of these input data can vary substantially (e.g., Garner, Malcolm, Sadler, & Hannah, 2014; Loicq, Moatar, Jullian, Dugdale, & Hannah, 2018; Trimmel et al., 2018). Consequently, tree cover data are often a considerable source of uncertainty when modelling river temperature in forested reaches (Dugdale, Malcolm, & Hannah, 2019; Loicq et al., 2018). Given that scientists and practitioners are currently involved in both the planting (e.g., Davies-Colley, Meleason, Hall, & Rutherford, 2009; Guillozet, 2015; Holzapfel, Weihs, & Rauch, 2013) and removal (e.g., CASS, 2010; Kiffney, Richardson, & Bull, 2003) of riparian vegetation with a view to managing stream temperature and/or water quality, a better understanding of this uncertainty is important for accurately simulating the thermal response of rivers to management.

The majority of studies incorporating riparian shading in river temperature models have used GIS polygons to denote the 2D extent of tree cover (e.g., Chen, Carsel, McCutcheon, & Nutter, 1998; Cox & Bolte, 2007; Fabris, Malcolm, Buddendorf, & Soulsby, 2018; Sridhar, Sansone, LaMarche, Dubin, & Lettenmaier, 2004), with heights subsequently informed either by attributing sparse field measurements (e.g., Rutherford, Blackett, Blackett, Saito, & Davies-Colley, 1997; Theurer, Voos, & Miller, 1984) to the polygons or through look-up tables (e.g., Bond, Stubblefield, & Van Kirk, 2015; Trimmel et al., 2018) that relate tree height to species and/or stand age. Although such methods have been demonstrated to produce reasonable model performance metrics, the use of coarse GIS data can sometimes result in an imprecise representation of true riparian shading (Loicq et al., 2018), contributing to model uncertainty. To address these shortcomings, recent research has demonstrated the efficacy of remotely-sensed digital elevation products from LiDAR (e.g., Justice, White, McCullough, Graves, & Blanchard, 2017; Loicq et al., 2018; Wawrzyniak, Allemand, Bailly, Lejot, & Piégay, 2017) or structure from motion (SfM) photogrammetry (Dugdale et al., 2019) for parameterising the shading routines of process-based temperature models. These methods provide accurate and finely resolved (0.1–1 m) data on the extent and height of riparian tree cover and largely address the shortcomings of polygon-based approaches. However, such data can be either (a) costly to obtain (LiDAR) or (b) require specialist software and hardware to assemble (SfM). There also exists a third potential source of riparian tree cover data that occupies an intermediate ground between the GIS polygons and the finer LiDAR/SfM products, namely medium resolution (1–10 m) digital elevation products derived from conventional photogrammetric (Landmap & GetMapping, 2014) or interferometric synthetic aperture radar (IFSAR) approaches (Intermap Technologies, 2007). Given that such data are often freely available from national mapping agencies for entire countries and are generally of a reasonable horizontal and vertical accuracy, it is possible that such data may also be reasonably well-suited for parametrising the riparian shading routines of river temperature models. However, the ability of these data to generate reasonable predictions of tree height is largely unknown, and the authors are not aware of any current temperature modelling studies incorporating such data. Furthermore, despite the large potential differences between these different sources of riparian tree extent and height data, no one has yet conducted a systematic intercomparison of their utility for parameterising stream temperature models. Consequently, there is a concerning lack of information on the relative accuracy of temperature simulations resulting from these different approaches.

This paper presents the results of a study to assess the relative performance of river temperature models parameterised with riparian tree cover data from a variety of different sources. We implemented the Heat Source process-based temperature model (Boyd & Kasper, 2003) on a salmon stream in Scotland and systematically parameterised the model with tree cover from different sources, each time comparing simulated and observed water temperature from a series of loggers installed within the stream. Our specific objectives were

1. To parameterise a river temperature model using tree height data derived from a range of different geospatial datasets;
2. To compare how model performance varies between these different input tree height data and to what extent estimates of the "riparian woodland effect" vary as a function of input tree height data; and
3. To understand whether the choice of input tree height data influences the simulated addition or removal of tree cover and its impact on stream temperature (with a view to determining whether the choice of tree cover data affects management advice).

The findings of this study provide useful guidance on the advantages and limitations of different riparian woodland datasets for characterising shading in river temperature models.

2 | METHODS

2.1 | Study site

We conducted our study in the lower 2.2 km of the Girnock Burn, a tributary of the Aberdeenshire River Dee, Scotland (57.0515°N, 3.1048°W; Figure 1). Topography in the catchment ranges from 230 to 862 m above sea level, and geology consists of impermeable bedrock overlain with glaciofluvial sediments (Malcolm, Soulsby, Youngson, & Hannah, 2005). Prevailing meteorology is typical of the Cairngorm mountains, with mean daily air temperatures ranging

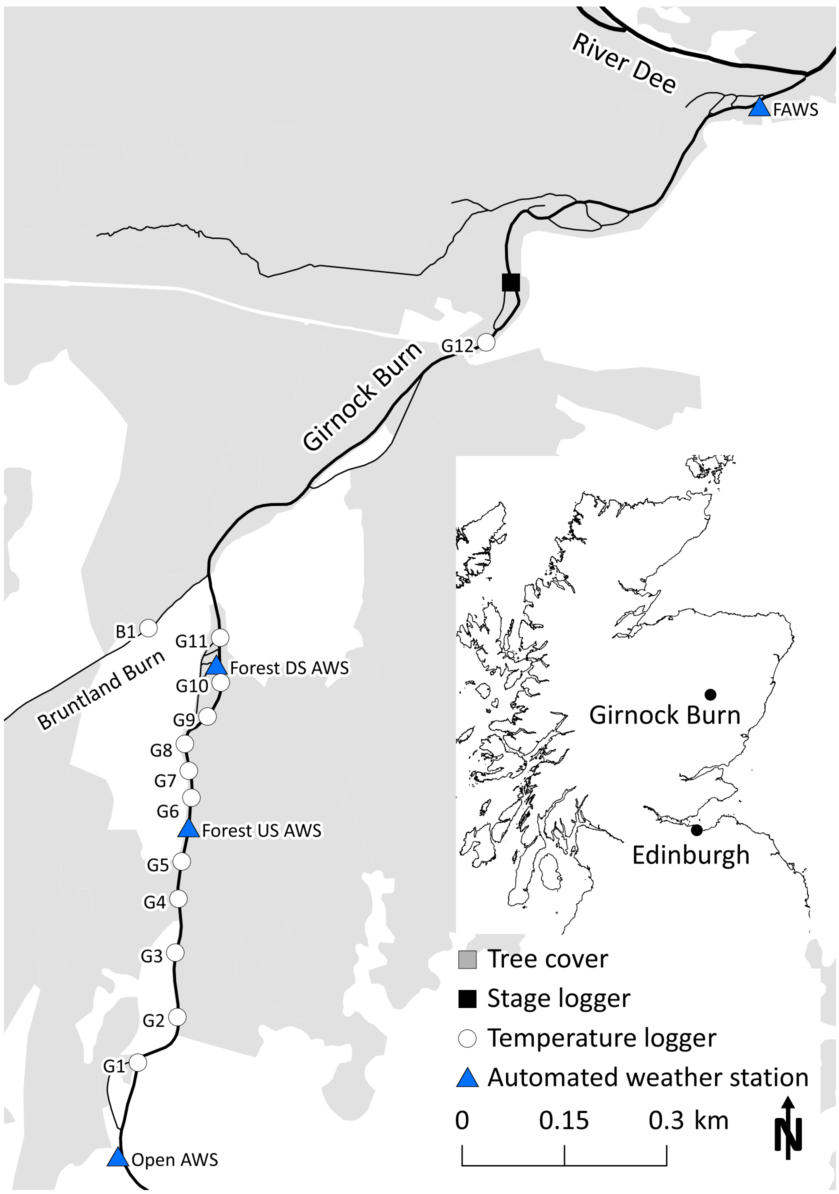

FIGURE 1 Girnock Burn study reach showing location of temperature loggers, automated weather stations and Marine Scotland gauging station

between 0.5–4.0°C in winter and 11.0–13.5°C in summer and a mean annual precipitation of ~1,100 mm (Hannah, Malcolm, Soulsby, & Youngson, 2004; Langan et al., 2001; Tetzlaff et al. 2005). Mean discharge within the Girnock Burn is 0.52 m^3 s^{-1} (Scottish Environmental Protection Agency gauging station gauge ID 12004). The study reach contains a transition from open heather moorland to seminatural deciduous woodland with small areas of commercial conifer plantation, typically set back from the riparian zone. Tree cover in the lower reach creates extensive shading that is known to have a significant moderating effects on stream temperature during the summer months (Garner et al., 2014; Hannah et al., 2008; Malcolm, Hannah, Donaghy, Soulsby, & Youngson, 2004). Further details of the study area can be found in Langan et al. (2001), Malcolm et al. (2005), Moir, Soulsby, and Youngson (2002) and Tetzlaff et al. (2005). Details of the riparian woodland characteristics can be found in Imholt, Soulsby, Malcolm, and Gibbins (2013).

2.2 | Temperature model

Heat Source Version 9.0.0b19 was used to simulate stream temperatures within the 2.2-km stretch of Girnock Burn. Heat Source is a process-based model that simulates river temperature as a function of input meteorological and hydromorphic data. It computes the gain (loss) of energy at each model node using the equation:

$$H_{\text{total}} = H_{sw} + H_{lw} + H_e + H_s + H_b + H_a, \tag{1}$$

where H_{total} is total energy gain (loss) by the river channel, H_{sw} is net shortwave radiation flux, H_{lw} is net longwave radiation flux, H_e is latent heat flux, H_s is sensible heat flux, H_b is heat conducted to or from the river bed, and H_a is advective flux from tributaries or groundwater/hyporheic exchange (all in watts per square metre). The contribution of these energy gains (losses) to stream temperature is calculated as a function of H_{total} and the volume, density, velocity, and specific heat capacity of water passing each model node at each timestep. In our implementation of Heat Source, H_{sw}, H_b, and the tributary inflow components of H_a were directly input into the model from field observations, whereas the remaining energy fluxes were simulated from input meteorological/hydromorphic data using routines contained within the model. For further details about Heat Source and the equations used to estimate the various heat fluxes, we refer the reader to Boyd and Kasper (2003) and Trimmel et al. (2018). More information on the specific implementation of Heat Source on the Girnock Burn can be found in Dugdale et al. (2019).

2.3 | Input data

2.3.1 | Field data

Heat Source was driven using hydrometeorological and geomorphological data relating to the 2.2-km study stretch of Girnock Burn. These data are outlined in detail in Garner et al. (2014) and Dugdale et al. (2019) and are available for download from Garner et al. (2018). In brief, meteorological data needed to run the model (i.e., air temperature (°C), relative humidity [percentage], wind speed [metre per second], incoming shortwave radiation, and bed heat flux [both Wm^{-2}]) were recorded at four automated weather stations located alongside the Burn (Figure 1). Geomorphic data (i.e., channel width, azimuth, and gradient) were measured from an orthophoto and digital elevation model of the site, whereas discharge was derived from a Marine Scotland Science stage logger installed at ~0.65 km upstream from the Burn's mouth (velocity-area rating curve R^2 = .97). Discharges were subsequently scaled by basin areas to drive both an upstream discharge boundary condition and an inflow for the Bruntland Burn, a small tributary that joins the Girnock Burn at 1.3 km upstream from its mouth. Velocities needed to calibrate Heat Source's hydraulic model predictions were derived from a discharge-mean-velocity function (Tetzlaff, Soulsby, Gibbins, Bacon, & Youngson, 2005) applied to the discharge data. The remaining model parameters needed to run Heat Source (e.g., streambed thermal conductivity, % hyporheic exchange, and Manning's coefficient) were tuned during model calibration (see Section 2.4).

2.3.2 | Tree cover data

Heat Source simulates the effect of riparian canopy shading on stream temperature by computing the attenuation of incoming solar radiation by vegetation (Boyd & Kasper, 2003). This is accomplished by supplying Heat Source with observations of vegetation height along a series of transects radiating out from each model node at 45° intervals (Figure 2); we used the *TTools* GIS package that accompanies Heat Source to sample vegetation using an along-transect spacing of 5 m (i.e., one sample of vegetation height/cover every 5 m from 5 to 45 m from the stream node). Heat Source then uses these data to calculate (for each timestep) the position of the sun along its arc relative to tree cover and, hence,

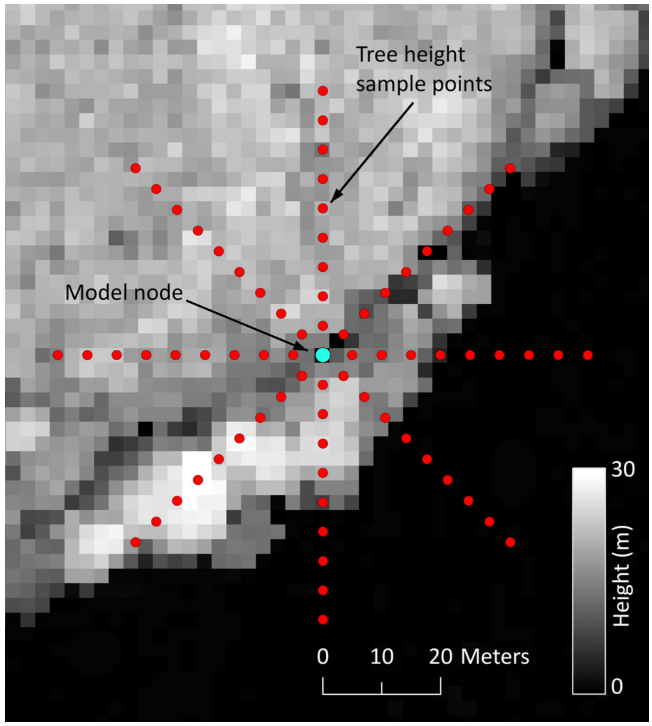

FIGURE 2 Schematic of tree cover input to Heat Source showing tree height sampling points superimposed on LiDAR tree height map

whether solar radiation will reach the stream or be blocked (direct H_{sw}) or attenuated (diffuse H_{sw}) by the canopy. Heat Source also computes the impact of tree cover on wind speed using the Prandtl–von Karman universal-velocity distribution law (Dingman, 2002) that approximates the frictional reduction in wind speed as a function of land cover height. Given that wind speed is a key determinant of turbulent heat fluxes, Heat Source thus simulates the effect of tree cover on latent (Q_e) and sensible (Q_s) heat gains (losses). In order to compare the performance of stream temperature simulations produced using different tree cover data, we successively parameterised Heat Source with data from six different geospatial datasets (as well as a "no trees" scenario to illustrate the impact of excluding tree height data from the model):

Structure from motion photogrammetry (SfM; 10 cm resolution; Figure 3a)

We used a small unoccupied aerial system (also known as a drone) to acquire ~3 cm aerial photography of the ~4 km by ~250 m area bounding the study reach. Agisoft PhotoScan Professional (Agisoft, 2017) was subsequently used to generate a 10 cm digital surface model (DSM) of the reach from the imagery. DSM accuracy was assessed as 0.11, 0.17, and 0.10 m (*x*-, *y*-, and *z*-coordinates, respectively) by calculating the root mean square error (RMSE) against 61 ground control points surveyed using a Leica Viva GS15 dGPS. We also used a Leica Viva TS12 total station (reflectorless mode) positioned overlooking the reach to measure the elevation of 64 tree crowns; comparison of these data against canopy elevations reconstructed from the SfM DSM showed a very good degree of correspondence (R^2 = .91). A SfM tree height map was subsequently

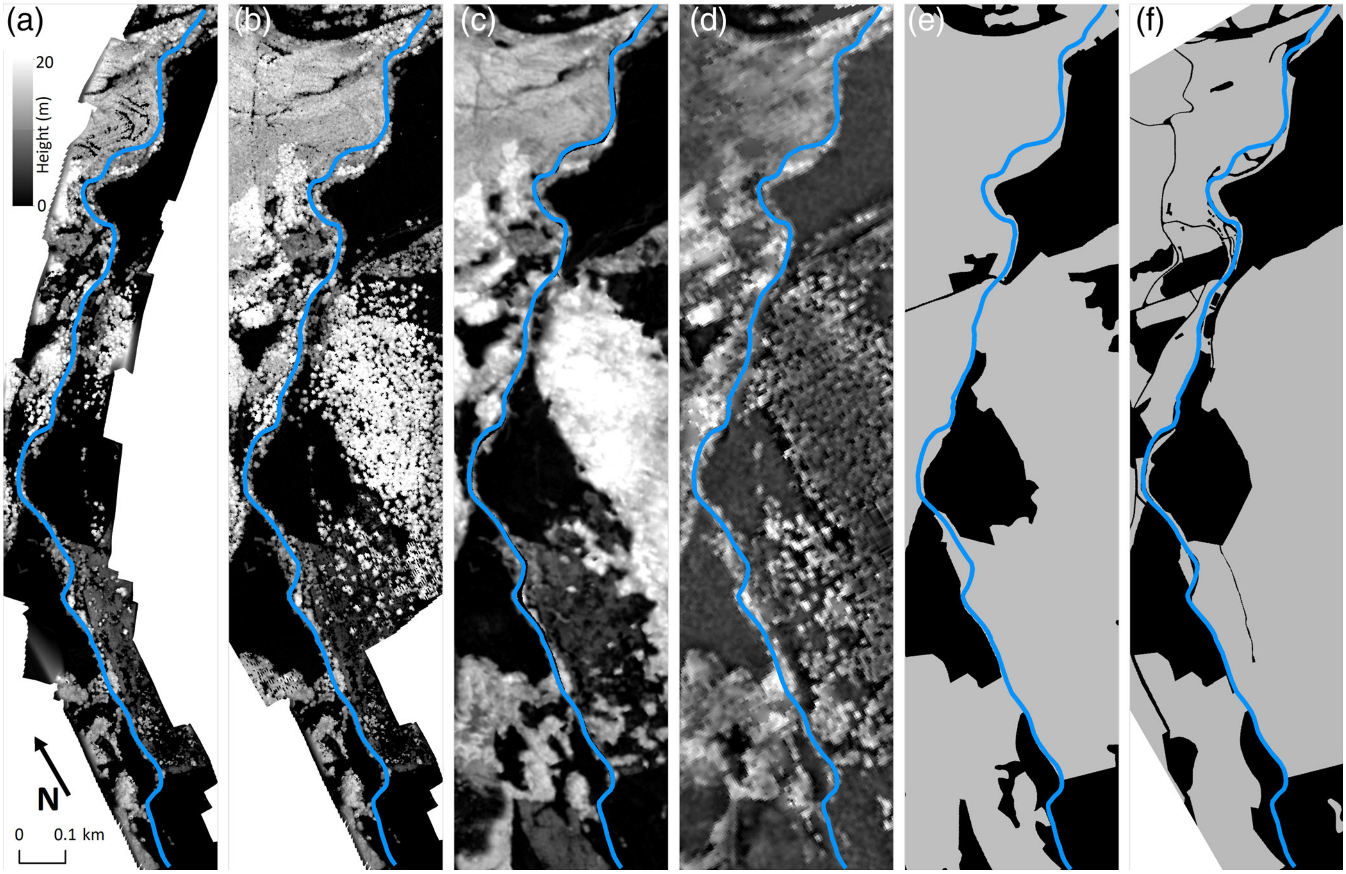

FIGURE 3 (a) SfM (b) LiDAR, (c) GetMapping, (d) NEXTMap, (e) NFI and (f) MasterMap tree height maps. Girnock Burn centreline denoted by blue line. Note north offset of −30°

calculated by subtracting a "bare earth" digital terrain model (DTM) from the DSM. The DTM was generated by using PhotoScan's point cloud classifier to identify ground points in the SfM dataset. For further details on the development of the SfM tree height map (including details on accuracy assessment of the bare earth DTM), we refer the reader to Dugdale et al. (2019).

LiDAR (1 m resolution; Figure 3b)

We obtained LiDAR data for the lower 1.7 km of Glen Girnock from the *LiDAR for Scotland Phase I* dataset (Scottish Government, 2012). The LiDAR data was separated into tree canopy points (LiDAR first returns) and ground points (last returns) and a DSM and DTM created from these datasets. Finally, a LiDAR tree height map was generated by subtracting the LiDAR DTM from the DSM. Because LiDAR data was only available for the lower ~1.7 km of Girnock Burn (rather than the full 2.2 km reach), we used elevations derived from the SfM dataset for the remaining ~0.5 km upstream section. Land use in this upper ~0.5 km section is predominantly open heather moorland, and the absence of LiDAR-derived tree height measurements for this location is therefore unlikely to have impacted results.

GetMapping photogrammetry (2 m DSM, 5 m DTM; Figure 3c)

Digital surface and terrain models derived using a "conventional" stereo photogrammetry approach (based on aerial photography) were obtained from the GetMapping 2 m DSM and 5 m DTM products downloaded from the Natural Environment Research Council Earth Observation Data Centre (Landmap & GetMapping, 2014). Although information regarding the bare earth DTM generation process is limited, details available at http://www.getmapping.com/support/height-lidar-data/how-digital-terrain-mode-dtm-height-data-produced (accessed June 19, 2018) indicate that the process involves the semiautomated classification of photogrammetric points into ground and nonground categories prior to raster DTM generation (stated vertical accuracy <60 cm RMSE). A tree height map (hereafter referred to as the GetMapping tree height map) was subsequently created by subtracting the the 5 m DTM (resampled to 2 m resolution) from the 2 DSM.

NEXTMap Interferometric Synthetic Aperture Radar (IfSAR; 5 m resolution; Figure 3d)

IfSAR-derived DSM and DTM rasters of the study area commissioned as part of the NEXTMap Britain programme (Intermap Technologies 2007) were used to create a 5 m tree height map (hereafter referred to as the NEXTMap tree height map) by subtracting the DTM from the DSM (after Scholefield et al., 2016). The NEXTMap DTM is derived using a proprietary algorithm (*TerrainFit*) that fits a bare earth surface to a multiresolution image "pyramid" of the original IfSAR DSM (Coleman & Mercer, 2002; Wang, Mercer, Tao, Sharma, & Crawford, 2001). Although this method produces a stated vertical accuracy (RMSE) of 60 cm in relatively flat/urban areas, reported accuracy in forested areas is lower (1.33–3.16 m; Wang et al., 2001), meaning that this error will likely propagate into the NEXTMap tree height map.

National Forest Inventory (NFI; GIS polygon; Figure 3e)

GIS polygons created as part of the UK Forestry Commission's National Forest Inventory (NFI) programme (Forestry Commission, 2017) delineate the spatial extent of riparian tree cover in the lower Girnock Burn. The NFI polygons are derived from manual interpretation of colour orthophotos taken within the preceding 3-year period and as such should be reasonably representative of current tree cover in Girnock Burn; the dataset covers all areas of contiguous woodland >0.5 ha. We selected all polygons in the following categories: *broadleaved*, *conifer*, *mixed (predominantly broadleaved)*, *mixed (predominantly conifer)*, and subsequently converted them to a 1 m raster. Raster pixels corresponding to the locations of the woodland polygons were assigned a uniform height of 10 m as this value closely approximated the mean nonzero tree height computed from the LiDAR and SfM tree height maps (9.95 and 9.79 m respectively). This dataset is hereafter referred to as the NFI tree height map.

Ordnance Survey MasterMap (GIS polygon; Figure 3f)

GIS polygons from the UK Ordnance Survey's MasterMap Topography Layer product (Ordnance Survey, 2018) were used to define the spatial extent of riparian tree cover. MasterMap tree cover is derived through manual orthophoto interpretation in a similar manner to the NFI data above; tree cover in our study section of Glen Girnock was last updated in 2014 and was therefore deemed representative of current tree cover in the Burn. We selected all polygons containing the terms *coniferous trees* or *nonconiferous trees* and converted them to a 1 m raster. Raster pixels corresponding to tree cover were again assigned a uniform height of 10 m (hereafter referred to as the MasterMap tree height map).

Prior to inputting these data to Heat Source, we also compared tree heights from the various datasets with a view to understanding the cause of potential variability between temperature model simulations. This was achieved through sampling the various tree height maps using a grid of points spaced at 10 m intervals within a 100 m buffer of the channel and then comparing them with the SfM dataset (determined to be the closest representation of true riparian tree height in Girnock Burn; see Dugdale et al., 2019). Only points that occurred under tree canopy (defined as >0.5 m in the SfM dataset) were sampled, to avoid the selection of bare ground elevations that would otherwise bias the comparison. We subsequently calculated the R^2 and RMSE between the SfM dataset and the other tree height maps.

2.4 | Model implementation and calibration

We implemented Heat Source on a 7-day period in July 2013 (July 1–7) characterised by relatively high air temperatures (15.6 ± 5.2°C) and low flows (0.12 m^3 s^{-1}). The model was used to simulate hourly water temperature at a streamwise resolution of 50 m. Wind speed, air temperature, and bed heat flux were assigned to each model node from the closest automated weather station whereas solar radiation was derived from only the upstream-most automated weather station (values unaffected by tree cover). Heat Source's shading routines subsequently enabled the generation of shade-corrected solar radiation fluxes and turbulent fluxes for each model node as a function of the various input tree cover data sources.

For the purposes of model calibration, Heat Source was parameterised using the SfM tree height map as this shading data was deemed to be the most accurate available. Calibration was achieved during a two-stage process. First, model calibration parameters (e.g., bed sediment conductivity, percentage hyporheic exchange, and wind function; see Boyd and Kasper (2003) for full list) were manually adjusted to minimise RMSE between simulated stream temperatures and temperatures observed at 14 water temperature observation sites located within the burn (12 TinyTag Aquatic 2 data loggers cross-calibrated to give accuracy of ±0.2°C and 2× Campbell Scientific 107 thermistor probes with accuracy of ±0.2°C); this manual phase allowed us to explore the parameter combinations that allowed the model parameters to stay within "real world" values. Model optimisation was achieved by iteratively searching 5,000 randomly-generated (via Latin hypercube sampling) parameter combinations falling within these real world values to find the combination that produced the optimum stream temperature simulation (i.e., the smallest RMSE value). Results of the calibration/optimisation process demonstrated that the Heat Source model (parameterised with the SfM tree height map) is able to reproduce stream temperature in the lower 2.2 km of the Girnock Burn with a very high degree of accuracy (RMSE ≈ 0.18–0.69°C; see Dugdale et al. (2019) for further details on model optimisation/calibration).

2.5 | Evaluation of model performance and sensitivity testing

2.5.1 | Comparing temperature model performance under varying tree cover data

Following calibration, the model was sequentially reparameterised with tree cover data from each of the sources detailed in Section 2.3.2. All other parameters optimised during model calibration were held constant to ensure that any variations in simulated temperature were solely the result of differences in the input tree cover data and not due to uncertainty in other model parameters. For each different tree height map, Heat Source was rerun for the simulation period detailed in Section 2.4. Model RMSE was again calculated at each of the 14 temperature observation sites; these data were subsequently tabulated to aid understanding of how differences in quality and resolution of input tree cover data impact the resulting stream temperature simulations.

2.5.2 | Simulating the addition and removal of riparian vegetation under varying tree cover data

In addition to characterising differences in model performance associated with the various tree height maps, we also conducted sensitivity testing to determine the suitability of the different geospatial datasets for simulating the effect of planting (addition of trees to a bare landscape) or clearcutting (removal of trees from an afforested landscape) on river temperature simulations. Specifically, we were interested in understanding the proximity to the river at which the addition or removal of riparian vegetation influences stream temperature, and whether the choice of tree height map affects these simulations. We accomplished this by successively adding (removing) tree height data to (from) the model at 5 m intervals (between 5 and 45 m) starting from the stream centreline and working outwards (Figure 2); the channel was sufficiently narrow to ensure that the innermost "ring" of tree cover (i.e., 5 m) was always located on the banks. Our decision to use an interval of 5-m stems from the fact that the crown diameter of mature deciduous and coniferous forest similar to that of the Girnock Burn usually exceeds 5 m (see Evans et al., 2015; Gill, Biging, & Murphy, 2000; Hemery, Savill, & Pryor, 2005; Pretzsch et al. 2015 for allometric data). Furthermore, 5 m corresponds to the horizontal spatial resolution of the coarsest dataset used in this study (NEXTMap tree height map) and was therefore chosen to ensure comparability between datasets. We subsequently calculated the reach-averaged RMSE and temperature for each tree height map at each 5-m step, aiding understanding of (a) proximity at which the addition (removal) of riparian vegetation has the largest impact on stream temperature and (b) to what extent the choice of input tree height data influences these simulations.

3 | RESULTS

3.1 | Accuracy of tree heights calculated from varying geospatial data

The tree height maps computed in Section 2.3.2 exhibit strong variability in calculated height (Figure 4). When compared with the SfM tree heights, the LiDAR-derived tree height map is most similar (R^2 = .61; RMSE = 3.25 m), with a coefficient of determination broadly similar to other studies comparing SfM and LiDAR-derived tree heights (e.g., Dandois & Ellis, 2010; Iglhaut et al., 2019; Wallace, Lucieer, Malenovský, Turner, & Vopěnka, 2016). Scatter in this relationship is presumably a function of the passage of time and seasonal differences between acquisition of the two datasets (see Dugdale et al., 2019). Visual inspection of the GetMapping tree height map (figure 3) indicates a reasonable degree of similarity with the SfM data (R^2 = .42; RMSE = 4.40 m). Closer analysis indicates that the increased error associated with this dataset (discussed further in Section 4.2) is likely due to the large number of "zero" tree heights in the GetMapping dataset. Contrary to these promising results, the NEXTMap dataset bears very little resemblance to the SfM data, with an extremely low coefficient of determination and greatly increased error (R^2 = .05). Unsurprisingly, the two polygon-based datasets (NFI and MasterMap tree height maps) also correlate poorly with the SfM data (R^2 = .10 and .04 respectively), given that tree heights within the "forest" polygons of these datasets were assigned a uniform value of 10 m. However, the RMSE associated with these tree height maps (6.54 and 5.35 m respectively) is nonetheless better than the NEXTMap dataset (8.80 m).

3.2 | Model performance under varying tree cover data

Results of the stream temperature simulations indicate that the Heat Source model of Girnock Burn performs best when parameterised using either the SfM or LiDAR-derived tree height maps (Table 1). This result is unsurprising given (a) the relative similarity of these datasets and (b) that the model was initially calibrated using the SfM dataset. The next-best-performing stream temperature model is that parameterised with the (GIS polygon-based) NFI tree height map, yielding only a small decrease in RMSE (8%) compared with the SfM/LiDAR-based models (RMSE = 0.51 vs. 0.47°C). However, despite this initially promising outcome for the "alternative" tree height maps, the remaining datasets performed markedly worse with a ~44–47% decline in RMSE to the next-best models (GetMapping and MasterMap). These models were characterised by similarly poor reach-averaged RMSE values of 0.68 and 0.69°C, respectively (Table 1), despite marked differences in provenance (i.e., photogrammetry-based tree heights vs. GIS polygons). The temperature model parameterised using the NEXTMap tree height map performed worst, with an RMSE in excess of 62% poorer than the best (SfM-derived) model. Nonetheless, even this result still compares favourably to the 'no trees model (RMSE = 0.86).

Although these reach-averaged RMSE values provide a broad indication of the performance of models parametrised from different tree cover data sources, closer inspection of the RMSE computed at each logger site reveals spatial patterns in model performance (Figure 5). As expected, the source of tree cover data makes little difference to model performance or mean temperature in the upper reach (2.2–1.9 km upstream from the confluence with the Dee) because tree cover in these upper reaches is almost entirely absent. However, in the lower reach (< 1.9 km from the Dee), the models start to diverge, coincident with an increase in forest cover. This divergence is apparent from increasingly different RMSE values between the various models (Figure 5a) but is most clearly evident in the time-averaged temperature series (Figure 5b). Indeed, although the models parameterised with the SfM, LiDAR, and NFI tree height maps yield similar stream temperature values even at the downstream end of the modelled reach, the MasterMap- and GetMapping-parameterised models display positive bias (overly warm values, although still cooler than the no trees model), whereas the NEXTMap model is negatively biased (excessive temperature loss). Taken together, this result suggests that although the models parameterised with the SfM, LiDAR, and NFI datasets are capable of adequately representing true stream temperature in the Girnock Burn, the other models are not adequate for this purpose.

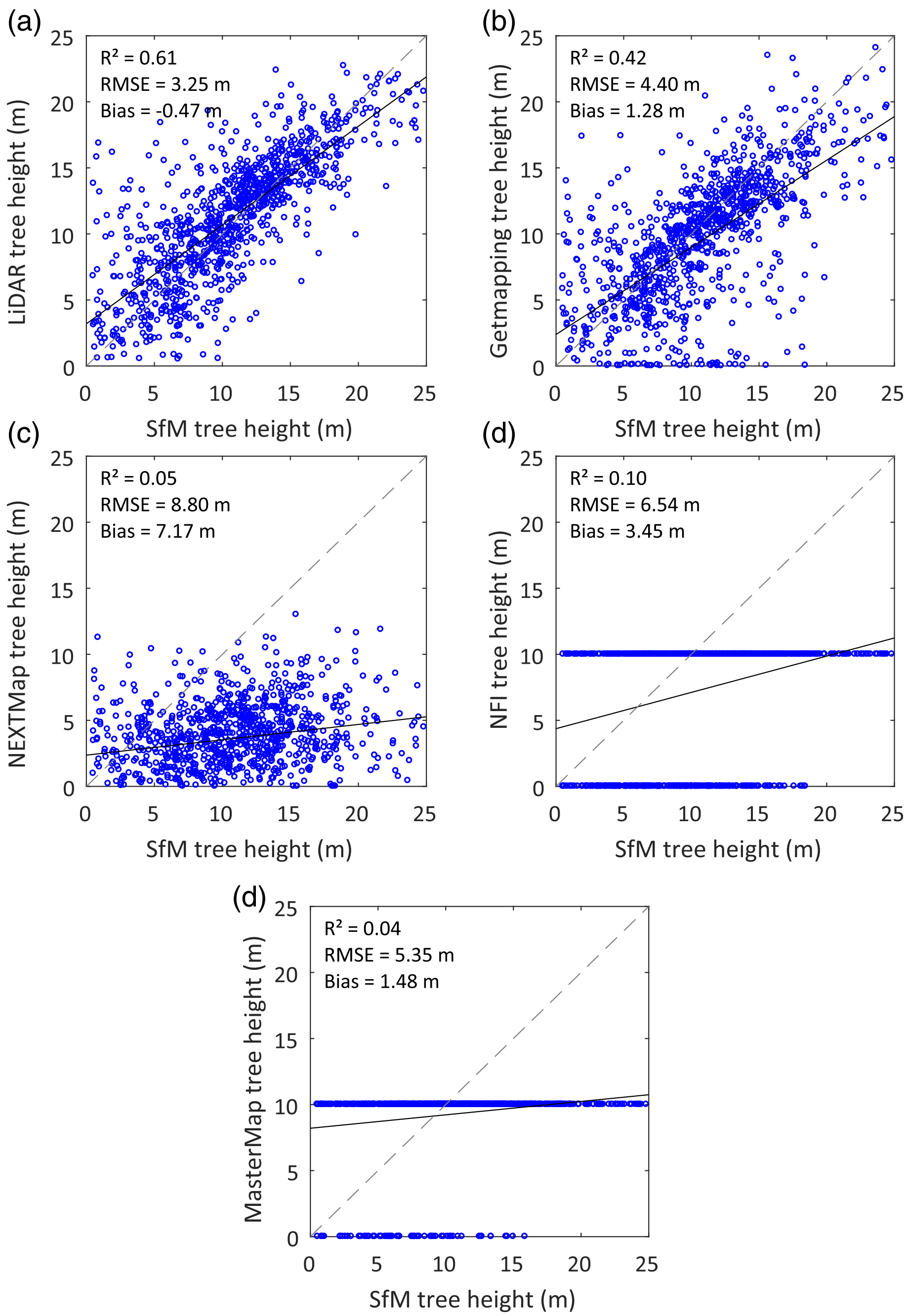

FIGURE 4 Comparison of heights from (a) LiDAR, (b) GetMapping, (c) NEXTMap, (d) NFI, and (e) MasterMap tree heights map against SfM dataset, considered to be the most accurate/up-to-date map of riparian tree heights in Girnock Burn. Tree heights for NFI and MasterMap datasets are either 0 m or 10 m based on values assigned to polygons. Linear regression shown as solid black line, grey dashed line gives 1:1

3.3 | Addition and removal of riparian vegetation

When tree cover data was systematically added to the riparian zone, model performance (as indicated by RMSE) improved most rapidly within 5 m of the channel, although smaller effects were still observed at distances of 10 m (Figure 6a). These results indicate that almost all of the effect of shading on stream temperature is generated by a relatively narrow strip of trees in close (≤10 m) proximity to the stream centreline. This finding is supported by the reach/time-averaged temperature data (Figure 6b) that also indicates that the overwhelming majority of stream temperature reductions occur where tree cover is added to the 5 and 10 m zones (with the addition of tree cover in subsequent zones not generating a substantial thermal response). Closer inspection of the individual models reveals that although the SfM, LiDAR, and NFI-parameterised models generated very similar trends in RMSE and stream temperature, the other models do not. Indeed, the NEXTMap model shows a substantial decrease in temperature with the addition of the tree cover within the 5 m zone, whereas results of the GetMapping and MasterMap-parameterised models suggest that the 10 m zone of tree cover generates a greater reduction in stream temperature (and hence, reduction in RMSE) than that the addition of tree cover at 5 m (which actually appears to generate a slight warming response). Taken together, these results indicate that models parameterised with these data perform poorly when used to simulate real data (see section 3.2) and that they are poorly suited to simulating “hypothetical” riparian tree planting scenarios.

TABLE 1 Average RMSE computed between 14 temperature observation sites and stream temperature model parameterised with given tree height map

Tree height map (resolution)	Reach-averaged RMSE (°C)	Standard deviation of RMSE (°C)	% decline in RMSE vs. best model
SfM (10 cm)	0.47	0.13	-
LiDAR (1 m)	0.47	0.13	0.01
NFI (GIS polygons)	0.51	0.25	8.0
Getmapping (2 m)	0.68	0.34	43.9
MasterMap (GIS polygons)	0.69	0.15	46.7
NEXTMap (5 m)	0.76	0.25	62.2
No trees	0.86	0.13	83.0

Unsurprisingly, results of the tree removal (clearcutting) scenarios largely mirrored those of the tree addition (Figure 7(a)). However, unlike the simulated addition of vegetation, the removal of vegetation from more distant zones (>10 m) continues to have a notable impact on stream temperature. Although the simulated removal of vegetation within the initial 5 m zone causes the largest deterioration in RMSE for the SfM, LiDAR, and NFI-parameterised models, the other models were characterised by little change or only marginal improvement in RMSE. Beyond 5 m, all models showed a similar deterioration in RMSE as vegetation was removed up to a distance of 15–20 m where RMSE values stabilised. In terms of the reach/time-averaged temperature data (Figure 7b), the SfM, LiDAR, and NFI-parameterised models show a steady increase in temperature associated with the removal of vegetation from each successive 5-m zone. However, the other models bely these results, with the removal of vegetation in the 5 m buffer strip actually causing a slight decrease in temperature for the MasterMap and GetMapping-parameterised models but a substantial increase for the NEXTMap model (essentially, an inversion of the results for the simulated addition of tree cover). This disparity again suggests that the NEXTMap, MasterMap, and GetMapping-

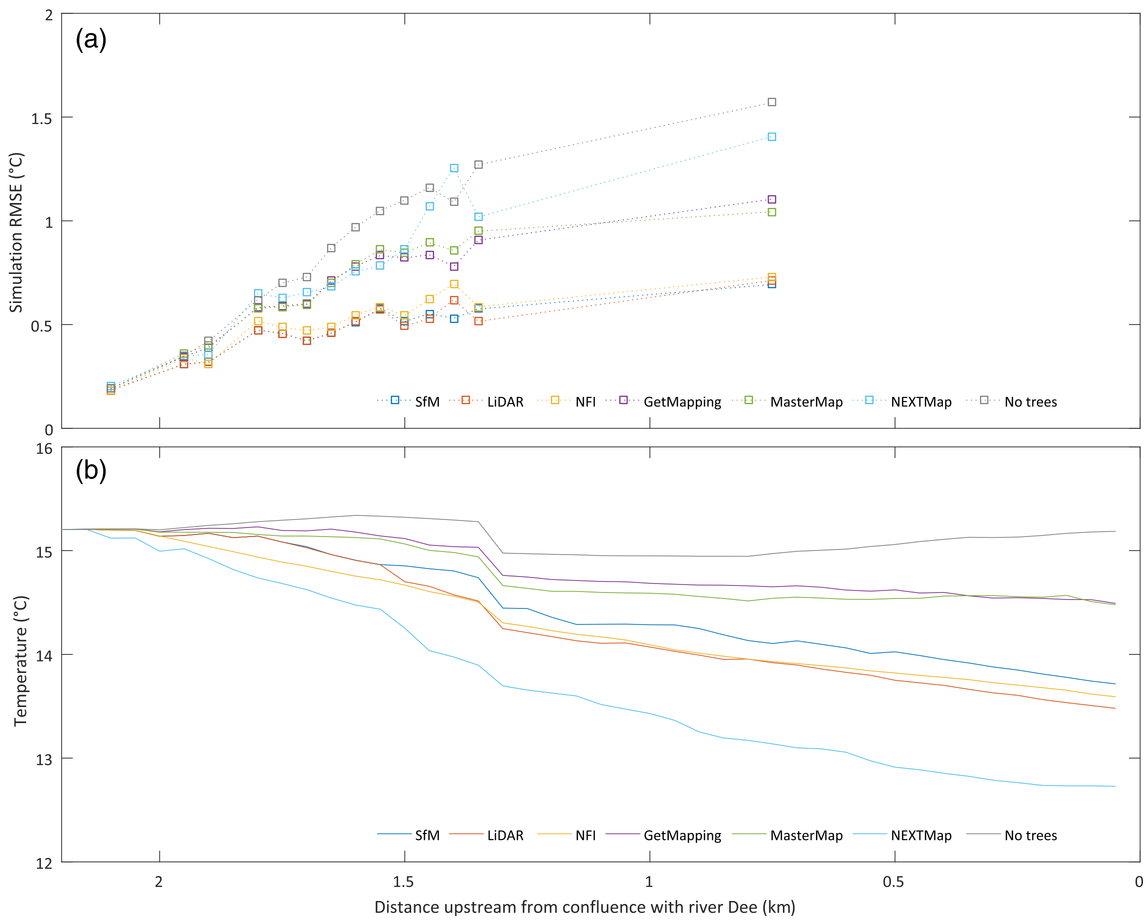

FIGURE 5 Variability in (a) streamwise RMSE computed against temperature loggers and (b) time-averaged stream temperature long profile generated by Heat Source model parameterised using various sources of tree cover data

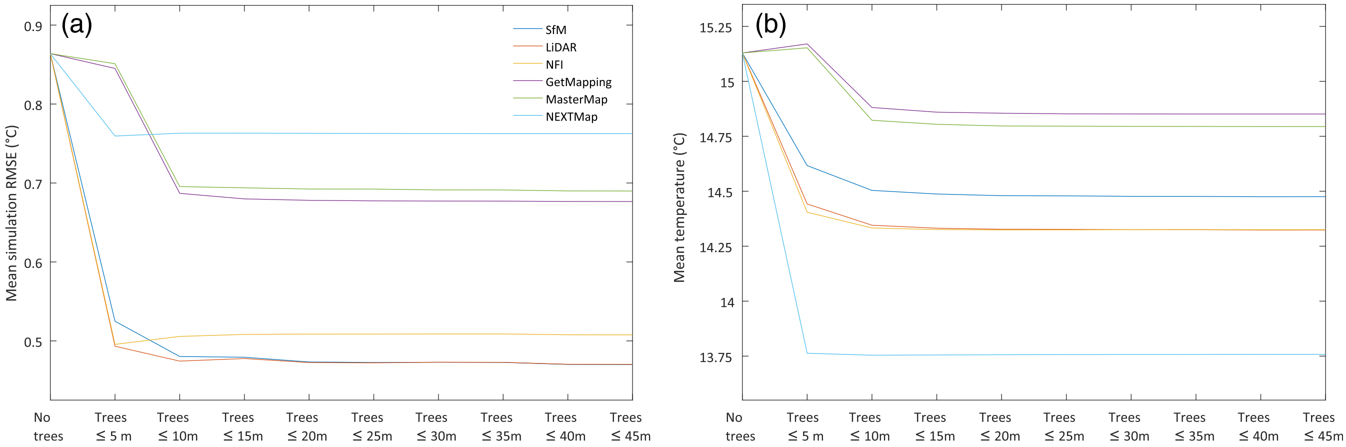

FIGURE 6 Tree planting simulation showing variation in (a) reach-averaged RMSE and (b) reach/time-averaged stream temperature produced by the addition of tree cover within successive 5 m zones for each Heat Source model

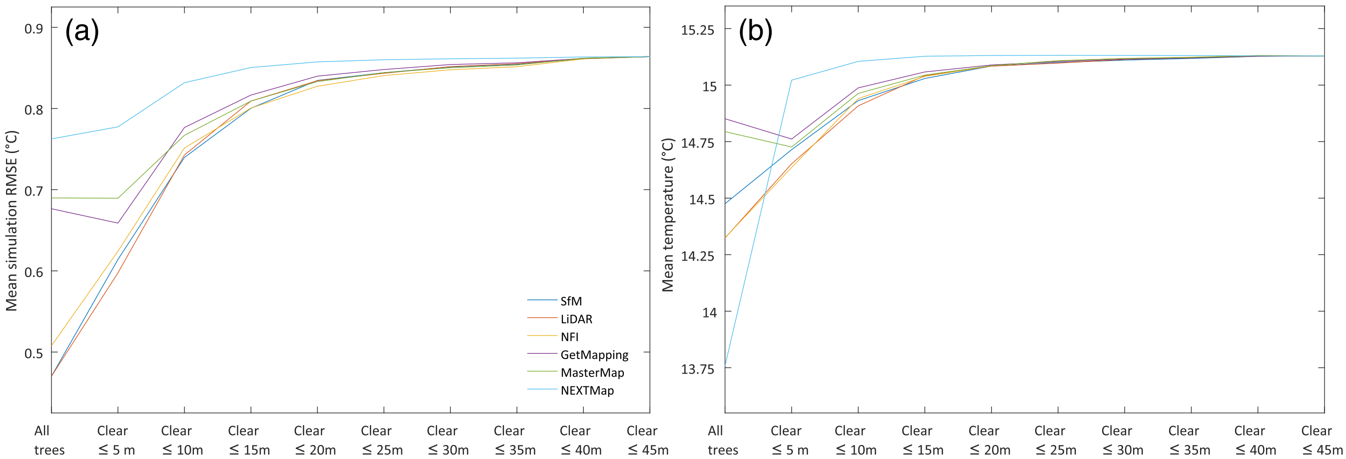

FIGURE 7 Clearcutting simulation showing variation in (a) reach-averaged RMSE and (b) reach/time-averaged stream temperature produced by the removal of tree cover from successive 5 m zones for each Heat Source model

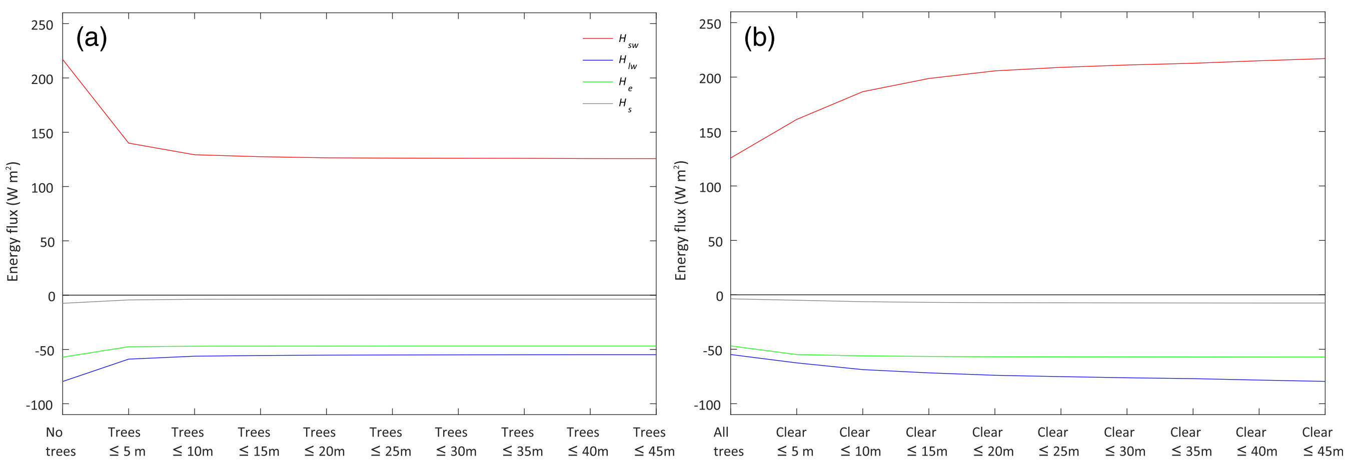

FIGURE 8 Reach-averaged shortwave, longwave, latent and sensible heat fluxes associated with (a) simulated tree cover addition and (b) simulated tree cover removal for best-performing Heat Source model (parameterised with structure from motion tree cover data)

parameterised models are less well-suited to simulating the hypothetical removal of riparian vegetation.

Patterns in the simulated radiative and turbulent heat fluxes associated with the best model (SfM) match patterns in the RMSE and temperature results for the tree planting and removal scenarios. In terms of tree planting, Figure 8a indicates that the bulk of the reduction of shortwave fluxes occurs within the 5 m riparian buffer strip closest to the channel, with subsequent "rows" of tree cover contributing relatively little to shortwave attenuation. In terms of tree removal (Figure 8b), shortwave radiation received at the stream surface steadily increases as a function of the removal of successive "strips" of vegetation up to distances of ~25–30 m either side of the channel. Longwave and turbulent heat fluxes show similar, but negative, trends. Interestingly, these results also show the impacts of tree cover addition on turbulent exchanges, with a reduction (increase) in latent and sensible heat fluxes associated with the addition (removal) of riparian shading. This likely reflects the fact that the cooler water temperatures engendered by shading will drive lower turbulent exchanges but is also partially due to routines within Heat Source that simulate the reduction in wind speed (and hence latent and sensible heat fluxes; see Section 2.3.2) under tree cover.

4 | DISCUSSION

4.1 | Influence of tree cover data source on model performance

Our investigation reveals that the type of tree cover data used to parameterise a stream temperature model can have a substantial impact on the quality of stream temperature simulations. Although this result is not unexpected, it is nonetheless illuminating that the use of "poorer" (in terms of both spatial resolution and height accuracy) riparian vegetation data (e.g., GetMappping, MasterMap, and NEXTMap) can generate an RMSE increase on the order of 40–60% as compared with the best-performing models. Although the good performance of the SfM and LiDAR models is not unexpected, the positive results generated by the NFI-derived model were somewhat surprising, given that this polygon-based tree height map is incapable of representing true spatial variability in riparian tree cover/height (see Figures 3e and 4d). Indeed, RMSE and stream temperature computed using the NFI-parameterised model were very similar to the LiDAR model, despite the complete absence of spatial variability in tree heights within the polygon dataset. Closer inspection of the NFI polygons reveals that this positive result is largely coincidental, and results from georeferencing inaccuracies that act to directly "overlay" the polygons on top of the Heat Source model nodes at key locations along the river (e.g., 1.5–2 km upstream). This "overlaying" causes positive tree heights to be assigned to the 5 m tree cover zone, which results in the NFI model simulating notably cool temperatures between 1.5 and 2 km. The net outcome of this is the generation of a very similar stream temperature signal to the SfM and LiDAR models. However, given that this positive result occurs almost entirely by chance due to "beneficial" georeferencing errors, it is unlikely that the NFI dataset would produce similarly-good results in other locations. Indeed, given the relatively poor results of the other polygon-based dataset (MasterMap) that did not incorporate similarly fortuitous spatial referencing errors, these findings indicate that GIS polygons should not be relied upon to generate detailed estimates of riparian shading (and the subsequent stream temperature response).

Unsurprisingly, even the poorest models (i.e., GetMapping, MasterMap, and NEXTMap) produced models with improved RMSE over the no trees scenario. Although this may suggest that using alternative tree cover data (of low resolution or height accuracy) is preferable to ignoring the presence of trees, we would urge caution. For example, although the GetMapping and MasterMap datasets show a plausible reduction in stream temperature (and associated improvement in RMSE) compared with the no trees model, the NEXTMap-derived model generates a substantially greater downstream cooling than is actually present in reality (see Section 4.2 for explanation). As a result, we do not advocate the use of these alternative data sources for parameterising the shading routines of stream temperature models, unless the simulated temperature response can be conclusively demonstrated to provide a good analogue of true river temperature.

4.2 | Performance of alternative tree cover datasets

In addition to the unexpectedly good performance of the NFI-derived model, the stream temperature models parameterised with alternative tree height data generated other unforeseen results. Of primary interest is the relatively poor performance of the GetMapping-derived model. Visual inspection of the tree height maps (Figure 3) indicates that the GetMapping-derived tree heights are relatively similar to those of the SfM and LiDAR datasets, a fact also supported by the reasonable correlation and RMSE (Figure 4). We were therefore surprised that this model generated considerably poorer stream temperature predictions. However, close inspection of the initial GetMapping raster shows that the river channel has been clipped from the input DSM/DTM using a buffer of ~5 m. This means that tree cover in the 5 m "zone" is generally absent within the resulting stream temperature model (apart from at a few sporadic locations where sampling nodes fall outside of this buffer). Given our finding that the majority of the tree shading effect on stream temperature occurs due to vegetation within this initial 5-m zone, it is therefore unsurprising that the performance of this model was suboptimal. The absence of vegetation in the 5 m zone also explains why the GetMapping-derived model showed the bulk of temperature reduction occurring with the addition of trees in the 10 m zone. Unfortunately, attempts to obtain an "unclipped" DSM/DTM product were unsuccessful, and it was therefore not possible to ascertain the performance of an unmodified GetMapping tree height map.

This general absence of trees in the 5-m zone also explains the similar performance of the MasterMap-derived model (compared with the NFI dataset) and accounts for the minor (but unexpected) warming noted as a result of the simulated addition of vegetation within the 5 m zone for the MasterMap and GetMapping models (Figures 6 and 7). Inspection of energy fluxes associated with tree planting (clearcutting) simulations (Figure 8) show that the addition of sporadic vegetation in this 5 m zone is accompanied by reduced windspeeds due to Heat Source's implementation of the Prandtl–von Karman universal-velocity distribution law that drive a decrease (increase) in turbulent losses. This, in combination with decreased longwave losses owing to the presence of bankside vegetation, offsets the shading-driven reduction in shortwave inputs thus causing the observed warming.

Turbulent fluxes also partially account for the anomalously high cooling observed in the NEXTMap-derived model. Average tree height computed from the NEXTMap data is considerably lower than from the other databases. Although this would normally mean that the shading effect is reduced in comparison with these other sources, the reduced tree height also drives an increase in turbulent losses that offsets a proportion of the reduction in shading-driven shortwave fluxes. However, these increased turbulent losses are not able to account for all of the observed cooling. Instead, the anomalously cool temperature is also a function of inaccuracies in the NEXTMap dataset that mean that the model is parameterised with falsely low height values for "emergent vegetation" (i.e., vegetation growing from within the channel or on point bars, etc.; see Boyd & Kasper, 2003). The presence of this artificially low emergent vegetation essentially acts as a "parasol" over the river channel, blocking a moderate amount of direct solar radiation at all hours of the day, rather than a larger amount of radiation over only 2–3 hours (as is generally the case with taller vegetation), thus explaining the excessive reduction in stream temperature.

Taken together, these findings demonstrate that process-based stream temperature models may behave in an unexpected manner when parameterised with unsuitable or inaccurate riparian vegetation data and may even generate results that, due to the way in which the model is programmed, do not have any real physical basis. As a result, we urge caution when working with coarser or less accurate tree height products and again stress that when their use is unavoidable, particular attention is paid to ensuring that simulated temperatures are reasonable and physically plausible.

4.3 | Implications of findings for river management

Our findings emphasise the importance of using high quality riparian vegetation data (in terms of spatial resolution and height accuracy) to parameterise process-based models of stream temperature. This is of particular importance when devising thermal management strategies for climate change to ensure that proposed management activities do not generate unwanted consequences. Indeed, the results of our tree planting/clearcutting simulations highlight that even when modelling "conceptual" land cover scenarios (as opposed to real world situations), the injection of realistic tree height data is essential in order to minimise unexpected model results or scenario outcomes (see Section 4.2; Figures 6 and 7).

The results of our tree planting/clearcutting scenario simulations using SfM or LiDAR data provide useful information for river managers wishing to implement river temperature management strategies. In terms of tree planting, our results indicate that the bulk of the tree shading effect on stream temperature occurs with the addition of trees in the initial 5 m zone alongside the river channel, confirming the results of Garner, Malcolm, Sadler, and Hannah (2017) and Malcolm et al. (2008) that indicate that the addition of a narrow "strip" of riparian vegetation only one to two trees in width can constitute an effective method for moderating temperature extremes. The knowledge that relatively narrow strips of riparian planting are able to produce reasonable stream temperature outcomes is also useful with regards to achieving a compromise between the competing demands of river managers (who are tasked with maintaining water temperature within optimal limits) and landowners/farmers (who want to minimise the loss of useable agricultural land to buffer strips), while simultaneously accomplishing maximum tree planting effectiveness within limited financial constraints. However, given that in the UK (and possibly other jurisdictions), it is often easier to obtain financing for the planting of woodland "blocks" rather than buffer strips (due in part to the higher fencing costs and lower woodland production associated with strips; Scottish Government, 2018), our findings regarding a single narrow strip of riparian planting may nonetheless require compromises to be made alongside other logistical concerns when conducting tree planting.

In terms of clearcutting, our results are of lesser relevance to agroforestery activities (e.g., Moore, Spittlehouse, & Story, 2005) that are generally compelled by legislation to leave a riparian buffer strip in excess of the 5 m limit discussed above (e.g., Davies, Biggs, Williams, & Thompson, 2009; González et al., 2017; Lee, Smyth, & Boutin, 2004). However, our findings have significant implications for jurisdictions where riparian buffers are actively managed (i.e., felling of riparian woodland) to *increase* mean temperature with a view to improving productivity or taxonomic richness (e.g., CASS, 2010). Results of our tree removal scenarios actually indicate that removal of just a single strip of vegetation located nearest to the river channel may only drive a relatively moderate increase in temperature. Indeed, to maximise the impact of clearcutting on stream temperature, it may therefore be necessary to fell trees as distant as 15–20 m from the channel centreline, presumably because even when located further from the channel, tall trees are able to generate substantial amounts of shading. Taken together, these results provide further information regarding riparian buffer management strategies for moderating stream temperature and add to the growing body of literature looking to better understand the nested drivers of stream temperature heterogeneity.

5 | CONCLUSIONS

River scientists and managers are increasingly using riparian tree planting to moderate high summer river temperatures with a view to mitigating some of the expected impacts of climate change. However, understanding the exact impacts of these activities requires simulation experiments within process-based stream temperature models. The results of our study show that, unless parameterised with high quality riparian tree cover data, such models are unable to adequately represent the effects of riparian shading on stream temperature. Indeed, when parameterised with suboptimal tree cover data, models not only generate less accurate temperature simulations, but may also act unexpectedly, producing unforeseen temperature outcomes. In our study, SfM and LiDAR tree cover data produced the best-performing stream temperature simulations, with alternative tree height sources generating suboptimal temperature simulations. This reduction in simulation quality results predominantly from inadequacies in their georeferencing and tree height data rather than as a function of their reduced spatial resolution. Were these georeferencing and height errors to be negated, it is plausible that these coarser data would produce stream temperature simulations approaching a similar (but lower) accuracy to those of the SfM and LiDAR tree cover. However, river scientists or managers should nevertheless look to use the tree cover data of the highest possible resolution and accuracy, with a view to producing optimal climate change adaptation strategies.

ACKNOWLEDGEMENTS

This project has received funding from the European Union's Horizon 2020 research and innovation programme under the Marie Skłodowska-Curie Grant Agreement No. 702468. IAM's contribution forms part of Marine Scotland Service Level Agreement FW02G. We wish to thank Stephen McLaren, Pauline Proudlock, Karen Millidine, Faye Jackson, and Ross Glover of Marine Scotland Science for help with SfM data collection. Small unoccupied aerial system surveys were conducted with the kind permission of the Abergeldie and Balmoral estates. We also thank Grace Garner for providing weather station and temperature logger data.

DATA AVAILABILITY STATEMENT

The data that support the findings of this study are available from a variety of sources: The weather station and temperature logger data were kindly made available by Grace Garner (Garner et al. 2018; downloadable from http://doi.org/10.7489/12109-1). The SfM data are available from the corresponding author upon reasonable request. The LiDAR data are Crown copyright Scottish Government, SEPA and Scottish Water (2012); Open Government Licence (http://www.nationalarchives.gov.uk/doc/open-government-licence/) and are available from the Scottish Remote Sensing Portal (https://remotesensingdata.gov.scot). The GetMapping data are copyright GetMapping (2014). The NEXTMap data are copyright Intermap Technologies (2007). Both of these datasets were downloaded from the NERC Earth Observation Data Centre (http://archive.ceda.ac.uk/). The NFI data contains, or is based on, information supplied by the Forestry Commission (2017) and is Crown copyright and database right Ordnance Survey (2018); these data are available from the Forestry Commission Open Data portal (http://data-forestry.opendata.arcgis.com/). The MasterMap data is Crown copyright and database right Ordnance Survey (2018) and was downloaded from the EDINA Digimap Service (http://digimap.edina.ac.uk/).

ORCID

Stephen J. Dugdale https://orcid.org/0000-0003-3561-4216
David M. Hannah https://orcid.org/0000-0003-1714-1240

REFERENCES

Agisoft. (2017). *Photoscan professional*. St. Petersburg, Russia: Agisoft LLC.

Battin, J., Wiley, M. W., Ruckelshaus, M. H., Palmer, R. N., Korb, E., Bartz, K. K., & Imaki, H. (2007). Projected impacts of climate change on salmon habitat restoration. *Proceedings of the National Academy of Sciences*, *104*, 6720–6725.

Bond, R. M., Stubblefield, A. P., & Van Kirk, R. W. (2015). Sensitivity of summer stream temperatures to climate variability and riparian reforestation strategies. *Journal of Hydrology: Regional Studies*, *4*(Part B), 267–279.

Bowler, D. E., Mant, R., Orr, H., Hannah, D. M., & Pullin, A. S. (2012). What are the effects of wooded riparian zones on stream temperature? *Environmental Evidence*, *1*, 3.

Boyd, M., & Kasper, B. (2003). *Analytical methods for dynamic open channel heat and mass transfer: Methodology for heat source model version 7.0*. Portland, OR: Oregon Department of Environmental Quality.

CASS. (2010). *Conservation of Atlantic Salmon in Scotland, final technical report (LIFE04NAT/GB/000250)*. Inverness: Scottish Natural Heritage.

Chen, Y. D., Carsel, R. F., McCutcheon, S. C., & Nutter, W. L. (1998). Stream temperature simulation of forested riparian areas: I. watershed-scale model development. *Journal of Environmental Engineering*, *124*, 304–315.

Coleman, M., & Mercer, J. (2002). NEXTMap Britain: Completing phase 1 of Intermap's global mapping strategy. *GeoInformatics*, *5*, 16–19.

Cox, M. M., & Bolte, J. P. (2007). A spatially explicit network-based model for estimating stream temperature distribution. *Environmental Modelling & Software*, *22*, 502–514.

Dandois, J. P., & Ellis, E. C. (2010). Remote sensing of vegetation structure using computer vision. *Remote Sensing*, *2*, 1157–1176.

Davies, B., Biggs, J., Williams, P., & Thompson, S. (2009). Making agricultural landscapes more sustainable for freshwater biodiversity: A case study from southern England. *Aquatic Conservation: Marine and Freshwater Ecosystems*, *19*, 439–447.

Davies-Colley, R. J., Meleason, M. A., Hall, R. M. J., & Rutherford, J. C. (2009). Modelling the time course of shade, temperature, and wood recovery in streams with riparian forest restoration. *New Zealand Journal of Marine and Freshwater Research*, *43*, 673–688.

Dingman, S. L. (2002). *Physical hydrology*. Long Grove, IL, USA: Waveland Press.

Dugdale, S. J., Hannah, D. M., & Malcolm, I. A. (2017). River temperature modelling: A review of process-based approaches and future directions. *Earth-Science Reviews*, *175*, 97–113.

Dugdale, S. J., Malcolm, I. A., & Hannah, D. M. (2019). Drone-based structure-from-motion provides accurate forest canopy data to assess shading effects in river temperature models. *Science of the Total Environment*, *678*, 326–340.

Evans, M. R., Moustakas, A., Carey, G., Malhi, Y., Butt, N., Benham, S., … Schäfer, S. (2015). Allometry and growth of eight tree taxa in United Kingdom woodlands. *Scientific Data*, *2*, 150006.

Fabris, L., Malcolm, I. A., Buddendorf, W. B., & Soulsby, C. (2018). Integrating process-based flow and temperature models to assess riparian forests and temperature amelioration in salmon streams. *Hydrological Processes*, *32*(6), 776–791.

Ficke, A., Myrick, C., & Hansen, L. (2007). Potential impacts of global climate change on freshwater fisheries. *Reviews in Fish Biology and Fisheries*, *17*, 581–613.

Forestry Commission (2017). National Forest Inventory Woodland Scotland. Forestry Commission, available at: http://data-forestry.opendata.arcgis.com/

Garner, G., Hannah, D.M., Dugdale, S.J., and Malcolm I. A. 2018. *Weather station, river temperature and discharge data from the Girnock burn in June-July* 2013. Marine Scotland Science, available at: http://doi.org/10.7489/12109-1

Garner, G., Malcolm, I. A., Sadler, J. P., & Hannah, D. M. (2014). What causes cooling water temperature gradients in a forested stream reach? *Hydrology and Earth System Sciences*, *18*, 5361–5376.

Garner, G., Malcolm, I. A., Sadler, J. P., & Hannah, D. M. (2017). The role of riparian vegetation density, channel orientation and water velocity in determining river temperature dynamics. *Journal of Hydrology*, *553*, 471–485.

Gill, S. J., Biging, G. S., & Murphy, E. C. (2000). Modeling conifer tree crown radius and estimating canopy cover. *Forest Ecology and Management*, *126*, 405–416.

González, E., Felipe-Lucia, M. R., Bourgeois, B., Boz, B., Nilsson, C., Palmer, G., & Sher, A. A. (2017). Integrative conservation of riparian zones. *Biological Conservation*, *211*, 20–29.

Guillozet, K. (2015). Shade trading: An emerging riparian Forest-based payment for ecosystem services market in Oregon, USA. *Environmental Management*, *56*, 957–970.

Hannah, D. M., Malcolm, I. A., Soulsby, C., & Youngson, A. F. (2004). Heat exchanges and temperatures within a salmon spawning stream in the Cairngorms, Scotland: Seasonal and sub-seasonal dynamics. *River Research and Applications*, *20*, 635–652.

Hannah, D. M., Malcolm, I. A., Soulsby, C., & Youngson, A. F. (2008). A comparison of forest and moorland stream microclimate, heat exchanges and thermal dynamics. *Hydrological Processes*, *22*, 919–940.

Hemery, G. E., Savill, P. S., & Pryor, S. N. (2005). Applications of the crown diameter–stem diameter relationship for different species of broadleaved trees. *Forest Ecology and Management*, *215*, 285–294.

Holzapfel, G., Weihs, P., & Rauch, H. P. (2013). Use of the shade-a-lator 6.2 model to assess the shading potential of riparian purple willow (*Salix purpurea*) coppices on small to medium sized rivers. *Ecological Engineering*, *61*, 697–705.

Iglhaut, J., Cabo, C., Puliti, S., Piermattei, L., O'Connor, J., & Rosette, J. (2019). Structure from motion photogrammetry in forestry: A review. *Current Forestry Reports*, *5*, 155–168.

Imholt, C., Soulsby, C., Malcolm, I. A., & Gibbins, C. N. (2013). Influence of contrasting riparian forest cover on stream temperature dynamics in salmonid spawning and nursery streams. *Ecohydrology*, *6*, 380–392.

Intermap Technologies (2007). NEXTMap British Digital Terrain Model Dataset Produced by Intermap. NERC Earth Observation Data Centre. Available at: http://catalogue.ceda.ac.uk/uuid/8f6e1598372c058f07b0aeac2442366d

Isaak, D. J., Wollrab, S., Horan, D., & Chandler, G. (2012). Climate change effects on stream and river temperatures across the northwest U.S. from 1980–2009 and implications for salmonid fishes. *Climatic Change*, *113*, 499–524.

Jonsson, B., & Jonsson, N. (2009). A review of the likely effects of climate change on anadromous Atlantic salmon Salmo salar and brown trout *Salmo trutta*, with particular reference to water temperature and flow. *Journal of Fish Biology*, *75*, 2381–2447.

Justice, C., White, S. M., McCullough, D. A., Graves, D. S., & Blanchard, M. R. (2017). Can stream and riparian restoration offset climate change impacts to salmon populations? *Journal of Environmental Management*, *188*, 212–227.

Kiffney, P. M., Richardson, J. S., & Bull, J. P. (2003). Responses of periphyton and insects to experimental manipulation of riparian buffer width along forest streams. *Journal of Applied Ecology*, *40*, 1060–1076.

Landmap & GetMapping (2014). GetMapping 2m resolution Digital Surface Model (DSM) for Scotland and Wales. NERC Earth Observation Data Centre. Available at: http://catalogue.ceda.ac.uk/uuid/4b0ed418e30819e4448dc89a27dc8388

Langan, S. J., Johnston, L., Donaghy, M. J., Youngson, A. F., Hay, D. W., & Soulsby, C. (2001). Variation in river water temperatures in an upland stream over a 30-year period. *Science of the Total Environment*, *265*, 195–207.

Lee, P., Smyth, C., & Boutin, S. (2004). Quantitative review of riparian buffer width guidelines from Canada and the United States. *Journal of Environmental Management*, *70*, 165–180.

Loicq, P., Moatar, F., Jullian, Y., Dugdale, S. J., & Hannah, D. M. (2018). Improving representation of riparian vegetation shading in a regional stream temperature model using LiDAR data. *Science of the Total Environment*, *624*, 480–490.

Malcolm, I. A., Hannah, D. M., Donaghy, M. J., Soulsby, C., & Youngson, A. F. (2004). The influence of riparian woodland on the spatial and temporal variability of stream water temperatures in an upland salmon stream. *Hydrology and Earth System Sciences*, *8*, 449–459.

Malcolm, I. A., Soulsby, C., Hannah, D. M., Bacon, P. J., Youngson, A. F., & Tetzlaff, D. (2008). The influence of riparian woodland on stream temperatures: Implications for the performance of juvenile salmonids. *Hydrological Processes*, *22*, 968–979.

Malcolm, I. A., Soulsby, C., Youngson, A. F., & Hannah, D. M. (2005). Catchment-scale controls on groundwater–surface water interactions in the hyporheic zone: Implications for salmon embryo survival. *River Research and Applications*, *21*, 977–989.

Moir, H. J., Soulsby, C., & Youngson, A. F. (2002). Hydraulic and sedimentary controls on the availability and use of Atlantic salmon (*Salmo salar*) spawning habitat in the river Dee system, north-east Scotland. *Geomorphology*, *45*, 291–308.

Moore, R. D., Spittlehouse, D. L., & Story, A. (2005). Riparian microclimate and stream temperature response to Forest harvesting: A review. *JAWRA Journal of the American Water Resources Association*, *41*, 813–834.

Ordnance Survey (2018). *MasterMap Topography Layer*. EDINA Digimap Service. Available at http://digimap.edina.ac.uk/

Pretzsch, H., Biber, P., Uhl, E., Dahlhausen, J., Rötzer, T., Caldentey, J., … Pauleit, S. (2015). Crown size and growing space requirement of common tree species in urban centres, parks, and forests. *Urban Forestry & Urban Greening*, *14*, 466–479.

Rutherford, J. C., Blackett, S., Blackett, C., Saito, L., & Davies-Colley, R. J. (1997). Predicting the effects of shade on water temperature in small streams. *New Zealand Journal of Marine and Freshwater Research*, *31*, 707–721.

Scholefield, P., Morton, D., Rowland, C., Henrys, P., Howard, D., & Norton, L. (2016). A model of the extent and distribution of woody linear features in rural Great Britain. *Ecology and Evolution*, *6*, 8893–8902.

Scottish Government (2012). LiDAR for Scotland Phase I. Scottish Government, SEPA and Scottish Water. Available at: https://remotesensingdata.gov.scot

Scottish Government (2018). Forestry Grant Scheme—Woodland Creation. Scottish Government Rural Payments and Services. Available at: https://www.ruralpayments.org/publicsite/futures/topics/all-schemes/forestry-grant-scheme/woodland-creation/

Seixas, G. B., Beechie, T. J., Fogel, C., & Kiffney, P. M. (2018). Historical and future stream temperature change predicted by a Lidar-based assessment of riparian condition and channel width. *JAWRA Journal of the American Water Resources Association*, *54*, 974–991.

Sridhar, V., Sansone, A. L., LaMarche, J., Dubin, T., & Lettenmaier, D. P. (2004). Prediction of stream temperature in forested watersheds. *JAWRA Journal of the American Water Resources Association*, *40*, 197–213.

Tetzlaff, D., Soulsby, C., Gibbins, C., Bacon, P. J., & Youngson, A. F. (2005). An approach to assessing hydrological influences on feeding opportunities of juvenile Atlantic Salmon (*Salmo salar*): A case study of two contrasting years in a small, nursery stream. *Hydrobiologia*, *549*, 65–77.

Tetzlaff, D., Soulsby, C., Youngson, A. F., Gibbins, C., Bacon, P. J., Malcolm, I. A., & Langan, S. (2005). Variability in stream discharge and temperature: A preliminary assessment of the implications for juvenile and spawning Atlantic salmon. *Hydrology and Earth System Sciences*, *9*, 193–208.

Theurer, F. D., Voos, K. A., & Miller, W. J. (1984). *Instream water temperature model. Instream flow information paper 16. FWS/OBS-84/15*. Washington, D.C.: US Fish and Wildlife Service.

Trimmel, H., Weihs, P., Leidinger, D., Formayer, H., Kalny, G., & Melcher, A. (2018). Can riparian vegetation shade mitigate the expected rise in stream temperatures due to climate change during heat waves in a human-impacted pre-alpine river? *Hydrology and Earth System Sciences*, *22*, 437–461.

Wallace, L., Lucieer, A., Malenovský, Z., Turner, D., & Vopěnka, P. (2016). Assessment of Forest structure using two UAV techniques: A comparison of airborne laser scanning and structure from motion (SfM) point clouds. *Forests*, *7*, 62.

Wang, Y., Mercer, B., Tao, V.C., Sharma, J., & Crawford, S. (2001). Automatic generation of bald earth digital elevation models from digital surface models created using airborne IFSAR. Proceedings of the 2001 ASPRS Annual Conference; pp. 23–27.

Wawrzyniak, V., Allemand, P., Bailly, S., Lejot, J., & Piégay, H. (2017). Coupling LiDAR and thermal imagery to model the effects of riparian vegetation shade and groundwater inputs on summer river temperature. *Science of the Total Environment*, *592*, 616–626.

How to cite this article: Dugdale SJ, Hannah DM, Malcolm IA. An evaluation of different forest cover geospatial data for riparian shading and river temperature modelling. *River Res Applic*. 2020;1–15. https://doi.org/10.1002/rra.3598